HHS Public Access

Author manuscript

Nature. Author manuscript; available in PMC 2011 July 13.

Published in final edited form as:

Nature. 2011 January 13; 469(7329): 250–254. doi:10.1038/nature09604.

ATM Damage Response and XLF Repair Factor are Functionally Redundant In Joining DNA Breaks

Shan Zha[1,2,*], **Chunguang Guo**[1,*], **Cristian Boboila**[1], **Valentyn Oksenych**[1], **Hwei-Ling Cheng**[1], **Yu Zhang**[1], **Duane R. Wesemann**[1], **Grace Yuen**[1], **Harin Patel**[1], **Peter H. Goff**[1], **Richard L. Dubois**[2], and **Frederick W. Alt**[1]

[1] Howard Hughes Medical Institute, The Children's Hospital, the Immune Disease Institute and the Harvard Medical School, Boston, MA 02115

Abstract

Classical non-homologous DNA end-joining (C-NHEJ) is a major mammalian DNA double strand break (DSB) repair pathway. Deficiencies for C-NHEJ factors, such as XRCC4, abrogate lymphocyte development, owing to a strict requirement for C-NHEJ to join V(D)J recombination DSB intermediates[1,2]. The XRCC4-like factor (XLF) is mutated in certain immunodeficient human patients and has been implicated in C-NHEJ[3,4,5,6]. Yet, XLF-deficient mice have relatively normal lymphocyte development and their lymphocytes support normal V(D)J recombination[5]. The Ataxia Telangiectasia-Mutated protein ("ATM") detects DSBs and activates DSB responses by phosphorylating substrates including histone H2AX[7]. However, ATM-deficiency causes only modest V(D)J recombination and lymphocyte developmental defects, and H2AX-deficiency does not measurably impact these processes[7,8,9]. Here, we show that XLF, ATM, and H2AX all have fundamental roles in processing and joining ends during V(D)J recombination; but that these roles have been masked by unanticipated functional redundancies. Thus, combined ATM/XLF-deficiency nearly blocks mouse lymphocyte development due inability to process and join chromosomal V(D)J recombination DSB intermediates. Combined XLF and ATM deficiency also severely impairs C-NHEJ, but not alternative end-joining, during IgH class switch recombination. Redundant ATM and XLF functions in C-NHEJ are mediated via ATM kinase activity and are not required for extra-chromosomal V(D)J recombination, suggesting a role for chromatin-associated ATM substrates. Correspondingly, conditional H2AX inactivation in XLF-deficient pro-B lines leads to V(D)J recombination defects associated with marked degradation of unjoined V(D)J ends, revealing that H2AX indeed has a role in this process.

Assembly of immunoglobulin (Ig) and T cell receptor variable region exons is initiated by the RAG1/2 endonuclease ("RAG"), which generates DNA DSBs between a pair of

Address Correspondence to: Frederick W. Alt (alt@enders.tch.harvard.edu).

[2]Current address: Department of Pathology and Cell Biology, Department of Pediatrics, Institute for Cancer Genetics, Columbia University, New York City, NY 10032

[*]These authors contributed equally to this work.

AUTHOR CONTRIBUTIONS

SZ, CG and FWA designed experiments and wrote the paper. SZ, CG, CB, VO, HC, YZ, DRW, GY, HP, PHG, RLD performed experiments.

participating V, D, or J coding segments and flanking recombination signal sequences (RSs)[10]. V(D)J recombination is completed via joining, respectively, of the two coding segments and two RSs by C-NHEJ[2]. While XLF-deficient ($XLF^{\Delta/\Delta}$) ES cells and mouse embryonic fibroblasts are impaired for V(D)J recombination of extra-chromosomal substrates[5], $XLF^{\Delta/\Delta}$ mice are only modestly impaired for lymphocyte development and $XLF^{\Delta/\Delta}$ pro-B lines, while IR-sensitive, perform nearly normal V(D)J recombination[5]. Thus, unknown factors may compensate for XLF V(D)J recombination functions in developing lymphocytes[5]. Among the candidates, we considered ATM, which is activated by RAG-generated DSBs[7,8,11]. To elucidate whether ATM has an overlapping V(D)J joining function with XLF, we bred $XLF^{\Delta/\Delta}$ mice[5] with ATM-deficient ($ATM^{-/-}$)[12] mice to generate $XLF^{\Delta/\Delta}ATM^{-/-}$ mice. $XLF^{\Delta/\Delta}ATM^{-/-}$ mice were live born but were significantly smaller than control littermates (Sup. Fig. 1).

$XLF^{\Delta/\Delta}$ and $ATM^{-/-}$ mice had only a modest (2–3 fold) reduction in thymocyte numbers and no gross alterations in thymocyte development as revealed by staining for the CD4 and CD8 differentiation markers (Fig. 1A,B, Sup. Tab. 1). In contrast, $XLF^{\Delta/\Delta}ATM^{-/-}$ mice had a greater than 20-fold decrease in thymocyte numbers, to levels nearly as low as those of $RAG2^{-/-}$ mice, with an overall developmental pattern reminiscent of that of certain C-NHEJ deficient mice with a “leaky” V(D)J recombination block[2]. B cell development also was relatively unimpaired in XLF- and ATM-deficient mice with both having only modestly reduced (2–3 fold) $B220^{+}IgM^{+}$ splenic B cell numbers (Fig. 1A,C, Sup. Tab. 1)[5,12]. In contrast, $XLF^{\Delta/\Delta}ATM^{-/-}$ mice had extremely low splenic B cell numbers (Fig. 1A,C, Sup. Tab. 1). Analyses of bone marrow B cell development in $XLF^{\Delta/\Delta}ATM^{-/-}$ mice suggested an impairment at the $CD43^{+}B220^{+}$ progenitor (pro-) B cell stage in which V(D)J recombination is initiated, as evidenced by the near absence of $B220^{+}CD43^{-}$ precursor B cells (Fig. 1A). To further test whether impaired B cell development in $XLF^{\Delta/\Delta}ATM^{-/-}$ mice involved a V(D)J recombination defect, we bred *IgH* and *IgL* loci that contained knock-in mutations of preassembled *IgH* and *IgL* variable region exons (referred to as “HL”)[13] into the $XLF^{\Delta/\Delta}ATM^{-/-}$ background and found a significant rescue of B, but not T, cell development (Fig. 1A,B,C and Sup. Tab. 1). Together, these findings suggest that XLF/ATM double-deficiency severely impairs T and B cell development by impairing V(D)J recombination.

To unequivocally test for V(D)J recombination end-joining defects, we generated *v-abl* transformed pro-B cell lines from WT, $XLF^{\Delta/\Delta}$, $ATM^{-/-}$, and $XLF^{\Delta/\Delta}ATM^{-/-}$ mice that carried bcl-2 transgenes[8]. Treatment of *v-abl* transformed pro-B lines with STI571, a *v-abl* kinase inhibitor, arrests cells in G1 and induces RAG, leading to efficient V(D)J recombination of integrated substrates in WT cells[8]. The bcl-2 transgene obviates apoptotic effects of STI571[8]. We generated multiple pro-B lines from each genotype that harbored, respectively, either a V(D)J recombination substrate designed to assay coding joins (CJs) and unjoined coding ends (CEs) (Fig. 2A) or a substrate designed to assay RS joins, (SJs), and unjoined RS ends (SEs) (Fig. 2B). For these experiments, DNA from individual lines was prepared at day 0 (before treatment), day 2, and day 4 of STI571 treatment, digested with restriction endonucleases and assayed for hybridization to indicated probes (Fig. 2C,D). WT and $XLF^{\Delta/\Delta}$ lines generated substantial CJ and SJ levels at day 2 and 4 with little or no obvious free CEs, indicative of a C-NHEJ defect (Fig. 2C,D). $ATM^{-/-}$ lines also generated

substantial levels of CJs and SJs; but, consistent with prior studies[8], also generated a modest level of unjoined CEs at day 2 that appeared partially resolved by day 4 (Fig. 2C). However, there was no obvious RS joining defect in the $ATM^{-/-}$ lines (Fig. 2D). In contrast, $XLF^{\Delta/\Delta}ATM^{-/-}$ lines had little accumulation of CJs or SJs at either time point and, instead, accumulated unjoined CEs and SEs, respectively (Fig. 2C,D).

We also tested for V(D)J recombination defects with a substrate that activates a GFP gene upon inversional V(D)J recombination and which, via Southern blotting, reveals CJs, hybrid joins (aberrant joins in which an RS is fused to a coding end), and free CEs (Fig 2E,F). We clonally integrated a single copy inversional V(D)J substrate into $XLF^{\Delta/\Delta}$ pro-B lines that were also homozygous for a conditional KO ATM allele ($ATM^{C/C}$)[12] and then deleted floxed $ATM^{C/C}$ sequences via Cre recombinase to generate $XLF^{\Delta/\Delta}ATM^{-/-}$ lines with the same substrate integration. Thus, these matched sets of lines allow assay of a given integrated substrate in $XLF^{\Delta/\Delta}$ pro-B lines before and after elimination of ATM. We treated inversional substrate containing WT, $ATM^{-/-}$, $XLF^{\Delta/\Delta}ATM^{C/C}$, $XLF^{\Delta/\Delta}ATM^{-/-}$ and $XRCC4^{-/-}$ lines with STI571 and assayed for V(D)J recombination both by GFP expression(Sup. Fig. 2) and Southern blotting (Fig. 2F). Both assays confirmed the severe V(D)J recombination defect in $XLF^{\Delta/\Delta}ATM^{-/-}$ pro-B lines and Southern blotting confirmed severely defective end-joining, as revealed by a dramatic decrease in CJs and a dramatic increase in unjoined CEs(Fig. 2F). The severity of the inversional V(D)J joining defect in $XLF^{\Delta/\Delta}ATM^{-/-}$ pro-B lines was similar to that of XRCC4-deficient pro-B lines (Fig. 2F and Sup. Fig. 2). $XLF^{\Delta/\Delta}$ pro-B lines treated with an ATM kinase inhibitor also showed a severe end-joining defect during V(D)J recombination, indicating that the ATM-mediated V(D)J joining activity revealed in XLF-deficient lines is mediated via ATM kinase activity(Fig. 2F). Finally, STI571-treated $XLF^{\Delta/\Delta}ATM^{-/-}$ pro-B lines accumulated unrepaired V(D)J recombination-associated breaks within their endogenous Igκ locus, similar to those observed in $Artemis^{-/-}$ pro-B lines, confirming that the V(D)J recombination defect associated with combined XLF and ATM deficiency extends to this endogenous Ig locus (Sup. Fig. 3).

To further characterize the V(D)J recombination defect in $XLF^{\Delta/\Delta}ATM^{-/-}$, versus WT, $XLF^{\Delta/\Delta}$, $ATM^{-/-}$ and $XRCC4^{-/-}$ pro-B lines, we assayed for V(D)J recombination on transiently introduced extrachromosomal substrates[14]. As this assay is semi-quantitative, within perhaps a 5-fold range, and is best for revealing profound defects, we performed at least 4 independent assays for each genotype (Sup. Table 1). As expected[2,5], transient coding and RS joining activity for XRCC4-deficient cells was more than 50-fold less than that of WT; while coding and RS joining activity for $XLF^{\Delta/\Delta}$ and $ATM^{-/-}$ cells approached the WT range (Sup. Table 2). Surprisingly, the range of coding and RS joining activity of $XLF^{\Delta/\Delta}ATM^{-/-}$ pro-B lines, while potentially modestly decreased, overlapped that of WT and single mutant cells (Sup. Table 2). Thus, in contrast to severe defects in chromosomal V(D)J recombination, XLF/ATM double mutant pro-B lines lack severe defects in extrachromosomal V(D)J recombination.

The chromosomal V(D)J joining defect in $XLF^{\Delta/\Delta}ATM^{-/-}$ pro-B lines can be attributed to impaired C-NHEJ, as V(D)J recombination exclusively employs this pathway[15]. However, the question remains as to whether $XLF^{\Delta/\Delta}ATM^{-/-}$ cells have more general C-NHEJ defects

and whether they are impaired for other forms of end-joining. *IgH* class switch recombination (CSR) involves introduction of DSBs into switch (S) region upstream of the Cμ constant region exons and their joining to DSBs within a downstream S region resulting in IgH CSR[16]. While C-NHEJ is a major CSR joining pathway, CSR occurs at reduced levels in C-NHEJ deficient cells via alternative end-joining (A-EJ)[13]. To assay CSR, we activated WT, $XLF^{\Delta/\Delta}$, $ATM^{-/-}$, and $XLF^{\Delta/\Delta}ATM^{-/-}$HL B cells for four days with anti-CD40 and interleukin 4 (IL-4) to stimulate CSR to IgG1. As expected[5,17,18,19,20], $XLF^{\Delta/\Delta}$ and $ATM^{-/-}$ B cells switched to IgG1 at about 40% of WT levels[5,17,18,19,20]. Moreover, $XLF^{\Delta/\Delta}ATM^{-/-}$HL B also showed substantial residual IgG1 CSR that was on average about 25% of WT levels (Fig. 3A,B; Sup Fig 4). To gain further insight into involved joining pathways, we sequenced the Sμ to Sγ1 junctions. C-NHEJ generates CSR junctions with no microhomology (*e.g.* direct joins) and junctions with short (1–2bp) microhomologies[13]; whereas A-EJ generates CSR junctions that predominantly contain microhomologies[13]. As expected, about 40% of WT junctions were direct[13]; while only about 22% and 13%, respectively, of $ATM^{-/-}$ and $XLF^{\Delta/\Delta}$ junctions were direct[5,20], suggesting some C-NHEJ impairment in these mutant B cells (Fig. 3C, Sup. Fig. 4). However, only about 5% of $XLF^{\Delta/\Delta}ATM^{-/-}$ CSR joins were direct (Fig. 3C, Sup. Fig. 4), consistent with most of their residual CSR being carried out by A-EJ. These results suggest that combined XLF and ATM deficiency impairs general C-NHEJ during CSR, but does not substantially impair A-EJ.

Our findings that the overlapping ATM function with XLF involves ATM kinase activity and is required for chromosomal versus extra-chromosomal V(D)J joining suggest this function involves ATM substrates. In response to DSBs, ATM phosphorylates H2AX[7]. However, H2AX-deficiency is not known to detectably impact V(D)J recombination[9,21]. To test for overlapping H2AX and XLF functions, we inter-crossed $XLF^{\Delta/\Delta}$ mice that were heterozygous for an inactivating mutation of H2AX[22] ($H2AX^{+/-}$). Surprisingly, these crosses yielded no $XLF^{\Delta/\Delta}H2AX^{-/-}$ pups, with embryonic death of double homozygous mutants occurring before embryonic day 13.5 (Table 1). The finding that combined XLF- and H2AX-deficiency, but not combined XLF- and ATM-deficiency, is embryonic lethal might have several explanations. One is that the lethality results from ATM-independent S phase functions of H2AX. Another is that impaired checkpoint functions associated with ATM deficiency rescue downstream effects of C-NHEJ deficiency that, otherwise, could result in embryonic death[23].

To determine whether XLF and H2AX have overlapping V(D)J recombination functions, we generated $XLF^{\Delta/\Delta}$ mice that were homozygous for a LoxP-flanked H2AX allele ($H2AX^{F/F}$)[21,22]. From these mice, we generated *v-abl* transformed $XLF^{\Delta/\Delta}H2AX^{F/F}$ pro-B lines containing an integrated single copy inversional V(D)J recombination substrate (Fig. 4A.B, Sup. Fig. 5). We then used Cre recombinase to generate matched sets of $XLF^{\Delta/\Delta}H2AX^{F/F}$ and $XLF^{\Delta/\Delta}H2AX^{-/-}$ lines, which were treated with STI571 and assayed for V(D)J recombination via GFP expression (Sup. Fig. 5). In six matched sets, each with a different substrate integration, H2AX deletion reduced, but did not eliminate, V(D)J recombination (Fig. 4A.B, Sup. Fig. 5), suggesting that XLF and H2AX also have overlapping V(D)J recombination activities, but not to the same extent as XLF and ATM. We also assayed for CJs, hybrid joins, and unjoined CEs by Southern blotting in 3 matched

sets of $XLF^{\Delta/\Delta}H2AX^{F/F}$ and $XLF^{\Delta/\Delta}H2AX^{-/-}$ pro-B lines (Fig. 4A.B, Sup. Fig. 4B). $XLF^{\Delta/\Delta}H2AX^{F/F}$ lines behaved like WT or $XLF^{\Delta/\Delta}$ lines, as they robustly generated CJs but not hybrid joins or unjoined CEs (Fig. 4A.B, Sup. Fig. 5). However, in accord with GFP assays, $XLF^{\Delta/\Delta}H2AX^{-/-}$ pro-B lines had substantially reduced CJs compared to $XLF^{\Delta/\Delta}H2AX^{F/F}$ parents; but, surprisingly did not show readily detectable unjoined CEs (Fig. 4A, B, Sup. Fig. 5).

Recent studies found that H2AX protects unjoined coding ends from ATM kinase and CtIP dependent resection[24]. To test whether reduced V(D)J recombination in $XLF^{\Delta/\Delta}H2AX^{-/-}$ pro-B lines resulted from reduced RAG cleavage or reduced joining of RAG cleaved ends coupled with end-resection, we performed V(D)J joining assays in $XLF^{\Delta/\Delta}H2AX^{F/F}$ and $XLF^{\Delta/\Delta}H2AX^{-/-}$ pro-B lines treated with ATM kinase inhibitor (Fig. 4A.B; Sup. Fig. 5). ATM inhibitor treatment of the $XLF^{\Delta/\Delta}H2AX^{F/F}$ lines reproduced the phenotype of $XLF^{\Delta/\Delta}ATM^{-/-}$ lines, including severely reduced CJs and the accumulation of unjoined CEs (Fig. 2F; Fig. 4A.B; Sup. Fig. 5). However, the ATM inhibitor-treated $XLF^{\Delta/\Delta}H2AX^{-/-}$ lines now yielded a clear band of unjoined CEs associated with a CE smear below the band that is characteristic of aberrant end resection (Fig. 4A.B; Sup. Fig. 5)[24]. To further examine this phenomenon, we used a sensitive TdT end labeling assay[24], which indeed revealed unjoined coding ends in STI571 treated $XLF^{\Delta/\Delta}H2AX^{-/-}$ pro-B lines without ATM inhibitor treatment (Sup. Fig. 6). These results demonstrate that XLF and H2AX have overlapping activities in V(D)J recombinational joining and also indicate that the unjoined V(D)J CEs in $XLF^{\Delta/\Delta}H2AX^{-/-}$ pro-B lines are largely resected in the absence of H2AX. As we did not find complete restoration of the unjoined coding ends in ATM kinase inhibitor treated $XLF^{\Delta/\Delta}H2AX^{-/-}$ pro-B lines, as was observed in ATM inhibitor-treated C-NHEJ-deficient cells that also are H2AX deficient[24], XLF might also have an overlapping function with H2AX in end-protection.

We consistently observed a lower level of TdT-labeled CEs in $XLF^{\Delta/\Delta}$ versus $XLF^{\Delta/\Delta}H2AX^{-/-}$ pro-B lines following STI-induction in the presence of ATM inhibitor, even though the latter have substantially higher levels of unjoined CEs (Fig. 4; Sup. Fig. 5 and 6). This finding suggested that unjoined CEs in ATM-inhibitor treated $XLF^{\Delta/\Delta}$ pro-B lines could be blocked from TdT activity. We employed urea denaturing gel electrophoresis to test for a defect in opening coding-end hair-pins and found ATM inhibitor-treated $XLF^{\Delta/\Delta}$ pro-B lines, like $Artemis^{-/-}$ but not $XRCC4^{-/-}$ lines, indeed accumulated unopened hair-pin CEs (Sup. Fig. 7). Given the overlapping functions of the ATM kinase and DNA-PK in CSR[25], plus the role of DNA-PK in activating Artemis to cleave hair-pin coding ends[2], it seemed possible that dual deficiency for ATM and XLF leads to a DNA-PK defect. However, measurements of ionizing-radiation induced phosphorylation of H2AX and KAP-1, both ATM and DNA-PK substrates[25], in the presence or absence of DNA-PK inhibitors, revealed DNA-PK kinase activity to be as active in $XLF^{\Delta/\Delta}ATM^{-/-}$ cells as in WT or $ATM^{-/-}$ cells (Sup. Fig. 8). However, we cannot rule out the possibility that $XLF^{\Delta/\Delta}ATM^{-/-}$ cells have a specific defect in DNA-PK activity in the context of V(D)J recombination joining that overlaps with ATM/XLF functions or that a DNA-PK defect in this context could represent a more general defect, for example in the broader recruitment of C-NHEJ factors. In the latter context, we note that the V(D)J recombination defect in

$XLF^{\Delta/\Delta}ATM^{-/-}$ pro-B lines is not just in hair-pin opening, since we also observe a severe defect in RS joining in these cells (Fig. 2).

ATM, XLF, and H2AX previously have been found to have, at most, modest roles in V(D)J recombination and, by extension, C-NHEJ [5,7,8,9]. Surprisingly, we now find that dual deficiency for XLF and ATM impacts V(D)J recombination in progenitor lymphocytes and IgH CSR in mature B cells similarly to deficiency for *bona fide* C-NHEJ factors. We conclude that XLF-deficient cells require ATM, and that ATM-deficient cells require XLF, to carry out C-NHEJ but not A-EJ. These findings further indicate that XLF-deficient cells provide a novel system for elucidating major, previously unappreciated roles of ATM and ATM substrates in C-NHEJ and *vice versa*. Indeed, our findings already suggest that XLF and ATM, via phosphorylation of its substrates, share overlapping functions primarily in the context of chromosomal C-NHEJ. We have also shown that the V(D)J recombination defects in XLF/ATM and XLF/H2AX deficient pro-B lines are not identical either in extent or in outcome. Thus, it remains possible that additional ATM substrates, besides H2AX, also may overlap functionally with XLF. XLF might directly influence the same processes as ATM or H2AX, including end processing and end resection, respectively. Alternatively, overlapping functions might be mediated indirectly through distinct processes. For example, XLF may influence reaction kinetics by C-NHEJ factor recruitment[26]; while ATM and ATM-substrates appear to tether chromosomal ends for joining[7,8], two distinct functions that theoretically could be redundant with respect to effects on overall joining activities.

METHODS

Mice

$XLF^{+/\Delta}$, $ATM^{+/-}$, $ATM^{+/C}$, $H2AX^{+/-}$ and $H2AX^{+/F}$ and "HL" mice have been described [5,12,21,22]. All HL mice were heterozygous for both *IgH* and *IgL* knockin alleles.

Chromosomal V(D)J recombination assays

V(D)J recombination with an integrated substrate was carried out as described[8]. Briefly, *v-abl* transformed pro-B-cell lines were isolated from various mouse lines that harbored an Eμ-Bcl2 transgene. For XRCC4-deficient *v-abl* transformants, the Eμ-Bcl2 transgene was introduced after establishment of the line[5]. The pro-B lines were infected with the pMX-INV, pMX-DelCJ or pMX-DelSJ retroviral vector and assayed for V(D)J recombination as described[5,8]. ATM inhibitor Ku55933 (Cat.No.118500 from EMD Biosciences) was used as a final concentration of 15μM as described[8].

Lymphocyte Development and Class Switch Recombination

Lymphocyte populations were analyzed by flow cytometry as described[5]. Isolation and activation of splenic B cells and flow cytometric assays were as described[13]. Sμ-Sγ1 junctions were isolated from day 4 anti-CD40 plus IL-4 stimulated B cells, cloned and sequenced as described[13].

Supplementary Material

Refer to Web version on PubMed Central for supplementary material.

Acknowledgments

We thank Yuko Fujiwara and Peiyi Huang for technical support. We thank Barry Sleckman for advice, reagents, and for critical review of this manuscript. This work is supported by NIH grant AI076210 to F.W.A. F.W.A. is an investigator of Howard Hughes Medical Institute. S.Z was a fellow, then senior fellow of Leukemia and Lymphomas Society of America and a St. Baldrick Scholar. C.G. and Y.Z are fellows of Cancer Research Institute. C.B. receives support from the pre-doctoral training program of Cancer Research Institute. DRW is supported by a career development award from AAAI/GlaxoSmithKline and by NIH training grant AI007376.

References

1. Lieber MR. The mechanism of human nonhomologous DNA end joining. J Biol Chem. 2008; 283:1–5. [PubMed: 17999957]
2. Rooney S, Chaudhuri J, Alt FW. The role of the non-homologous end-joining pathway in lymphocyte development. Immunol Rev. 2004; 200:115–131. [PubMed: 15242400]
3. Ahnesorg P, Smith P, Jackson SP. XLF interacts with the XRCC4-DNA ligase IV complex to promote DNA nonhomologous end-joining. Cell. 2006; 124:301–313. [PubMed: 16439205]
4. Buck D, et al. Cernunnos, a novel nonhomologous end-joining factor, is mutated in human immunodeficiency with microcephaly. Cell. 2006; 124:287–299. [PubMed: 16439204]
5. Li G, et al. Lymphocyte-Specific Compensation for XLF/Cernunnos End-Joining Functions in V(D)J Recombination. Mol Cell. 2008; 31:631–640. [PubMed: 18775323]
6. Zha S, Alt FW, Cheng HL, Brush JW, Li G. Defective DNA repair and increased genomic instability in Cernunnos-XLF-deficient murine ES cells. Proc Natl Acad Sci U S A. 2007; 104:4518–4523. [PubMed: 17360556]
7. Bassing CH, Alt FW. The cellular response to general and programmed DNA double strand breaks. DNA Repair (Amst). 2004; 3:781–796. [PubMed: 15279764]
8. Bredemeyer AL, et al. ATM stabilizes DNA double-strand-break complexes during V(D)J recombination. Nature. 2006; 442:466–470. [PubMed: 16799570]
9. Yin B, et al. Histone H2AX stabilizes broken DNA strands to suppress chromosome breaks and translocations during V(D)J recombination. J Exp Med. 2009; 206:2625–2639. [PubMed: 19887394]
10. Bassing CH, Swat W, Alt FW. The mechanism and regulation of chromosomal V(D)J recombination. Cell. 2002; 109 (Suppl):S45–S55. [PubMed: 11983152]
11. Bredemeyer AL, et al. DNA double-strand breaks activate a multi-functional genetic program in developing lymphocytes. Nature. 2008; 456:819–823. [PubMed: 18849970]
12. Zha S, Sekiguchi J, Brush JW, Bassing CH, Alt FW. Complementary functions of ATM and H2AX in development and suppression of genomic instability. Proc Natl Acad Sci U S A. 2008; 105:9302–9306. [PubMed: 18599436]
13. Yan CT, et al. IgH class switching and translocations use a robust non-classical end-joining pathway. Nature. 2007; 449:478–482. [PubMed: 17713479]
14. Gellert M. Molecular analysis of V(D)J recombination. Annu Rev Genet. 1992; 26:425–446. [PubMed: 1482120]
15. Corneo B, et al. Rag mutations reveal robust alternative end joining. Nature. 2007; 449:483–486. [PubMed: 17898768]
16. Chaudhuri J, et al. Evolution of the immunoglobulin heavy chain class switch recombination mechanism. Adv Immunol. 2007; 94:157–214. [PubMed: 17560275]
17. Franco S, et al. H2AX prevents DNA breaks from progressing to chromosome breaks and translocations. Mol Cell. 2006; 21:201–214. [PubMed: 16427010]
18. Ramiro AR, et al. Role of genomic instability and p53 in AID-induced c-myc-Igh translocations. Nature. 2006; 440:105–109. [PubMed: 16400328]

19. Lumsden JM, et al. Immunoglobulin class switch recombination is impaired in Atm-deficient mice. J Exp Med. 2004; 200:1111–1121. [PubMed: 15504820]
20. Reina-San-Martin B, Chen HT, Nussenzweig A, Nussenzweig MC. ATM is required for efficient recombination between immunoglobulin switch regions. J Exp Med. 2004; 200:1103–1110. [PubMed: 15520243]
21. Bassing CH, et al. Increased ionizing radiation sensitivity and genomic instability in the absence of histone H2AX. Proc Natl Acad Sci U S A. 2002; 99:8173–8178. [PubMed: 12034884]
22. Bassing CH, et al. Histone H2AX: a dosage-dependent suppressor of oncogenic translocations and tumors. Cell. 2003; 114:359–370. [PubMed: 12914700]
23. Sekiguchi J, et al. Genetic interactions between ATM and the nonhomologous end-joining factors in genomic stability and development. Proc Natl Acad Sci U S A. 2001; 98:3243–3248. [PubMed: 11248063]
24. Helmink BA, et al. H2AX Inhibits CtIP-Mediated DNA End Resection and Homology-Mediated DNA Repair in G1-Phase Cells. Nature. in press.
25. Callen E, et al. Essential role for DNA-PKcs in DNA double-strand break repair and apoptosis in ATM-deficient lymphocytes. Mol Cell. 2009; 34:285–297. [PubMed: 19450527]
26. Yano K, et al. Ku recruits XLF to DNA double-strand breaks. EMBO Rep. 2008; 9:91–96. [PubMed: 18064046]
27. Celeste A, et al. Genomic instability in mice lacking histone H2AX. Science. 2002; 296:922–927. [PubMed: 11934988]
28. Peitz M, Pfannkuche K, Rajewsky K, Edenhofer F. Ability of the hydrophobic FGF and basic TAT peptides to promote cellular uptake of recombinant Cre recombinase: a tool for efficient genetic engineering of mammalian genomes. Proc Natl Acad Sci U S A. 2002; 99:4489–4494. [PubMed: 11904364]

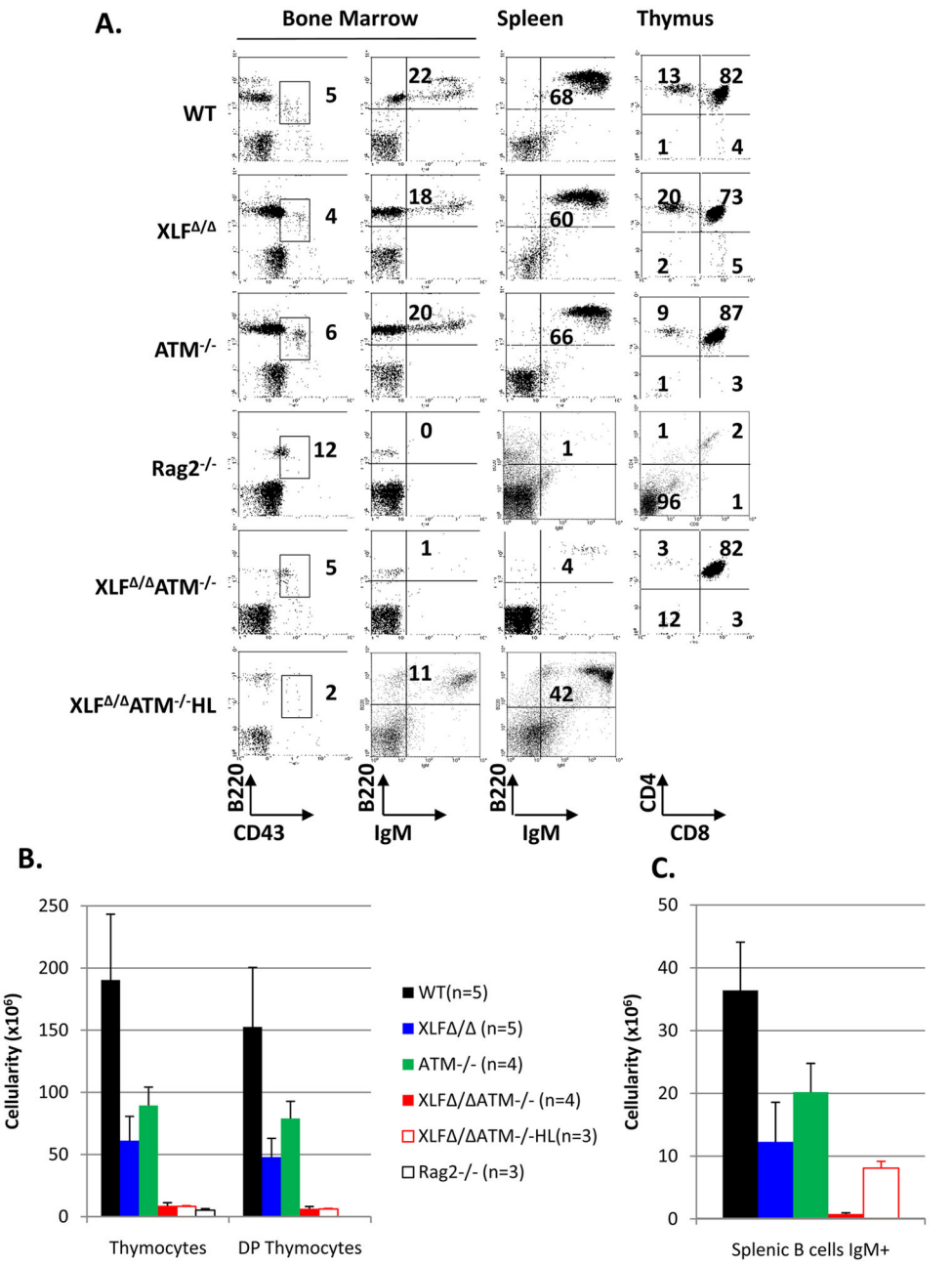

Figure 1. ATM and XLF have redundant functions in lymphocyte development

(A) Representative flow cytometric analyses of bone marrow, spleen and thymus from WT, $XLF^{\Delta/\Delta}$, $ATM^{-/-}$, $Rag2^{-/-}$, $XLF^{\Delta/\Delta}ATM^{-/-}$ and $XLF^{\Delta/\Delta}ATM^{-/-}$HL mice (see Method for further description of mouse lines). Numbers on the plot are percentage of total cells represented by indicated population. (B) Total thymocyte, DP thymocyte and (C) IgM^{+} splenic B cell numbers. Each value listed represents the average ± standard deviation from at least three mice between 4 to 12 weeks of age. Details are found in Supp. Tab.1.

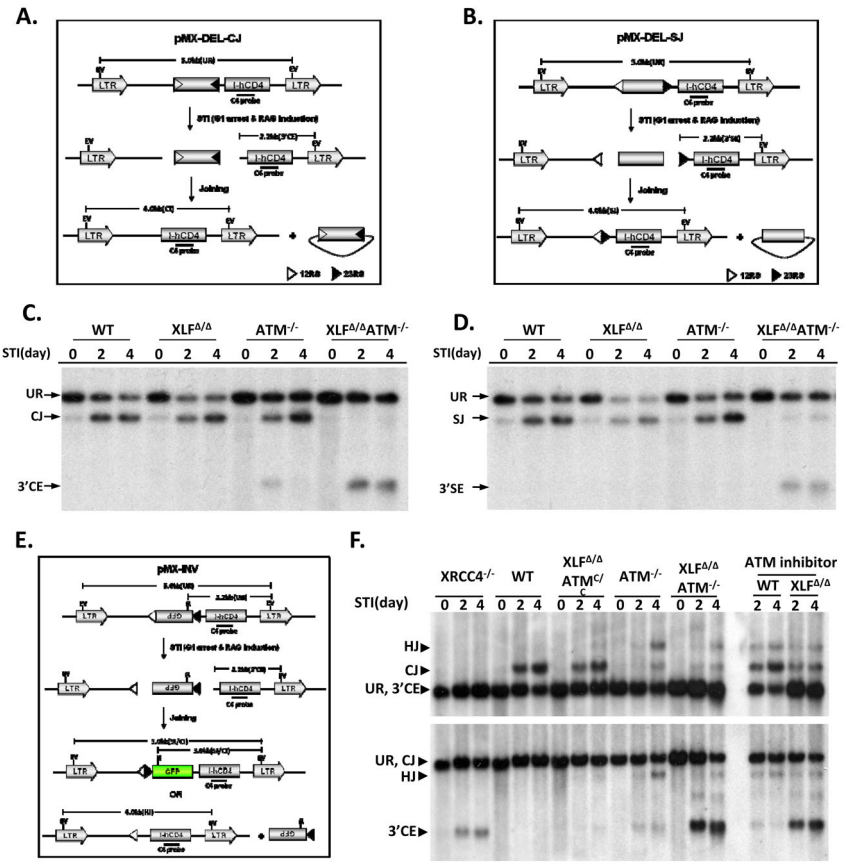

Figure 2. ATM and XLF have redundant functions in chromosomal V(D)J recombination

Schematic of pMX-DEL-CJ (A), pMX-DEL-SJ (B) and pMX-INV (E) retroviral recombination substrates designed to assay CJ, SJ, and inversional V(D)J recombination, respectively[8]. Diagrams indicate un-rearranged substrate (UR), coding/signal end (CE/SE) intermediates and coding/signal joints (CJ/SJ). The 12-RS (open triangle), GFP coding sequence, 23-RS (filled triangle), IRES-truncated hCD4 cDNA (I-hCD4) and LTRs are indicated. Positions of EcoRV (EV) sites, NcoI (N) sites and C4 probe (black bar) are shown. (C and D) Southern blotting with C4 probe of EcoRV-digested DNA from STI571 treated (2 or 4 days) *v-abl* pro-B lines containing pMX-DEL-CJ (C) or pMX-DEL-SJ (D) substrates. Results were obtained from cell pools with diverse substrate integrations. Similar results were obtained with single integration clones (not shown). Bands reflecting pMX-DEL-CJ UR, CE, CJ (panel C) and pMX-DEL-SJ UR, SE, SJ (panel D) are indicated. (F) Southern blot with C4 probe of EcoRV-NcoI digested (upper panel) or EcoRV digested (lower panel) DNA from indicated lines containing a single pMX-INV substrate. The XLF$^{\Delta/\Delta}$ATM$^{C/C}$ and the XLF$^{\Delta/\Delta}$ATM$^{-/-}$ lines have identical integrations. See legend to Supp. Fig. 5 for detailed methods.

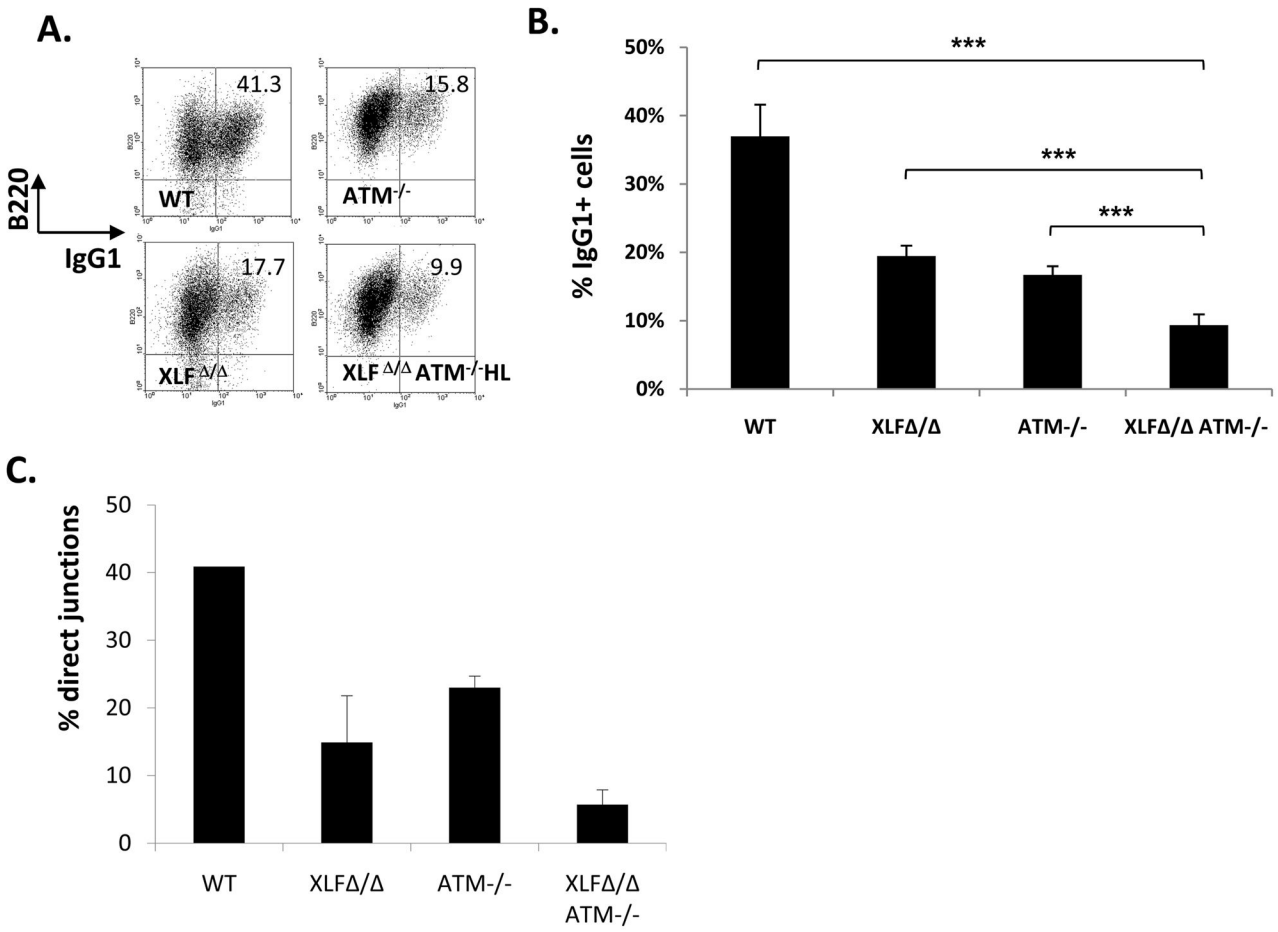

Figure 3. ATM and XLF synergize in C-NHEJ during CSR

(A) Representative flow cytometric analysis of (at least 3 independent experiments for each genotype) purified $CD43^-$ splenocytes from of indicated mice stained for surface B220 and surface IgG1 following a four-day stimulation with anti-CD40 and IL-4. Additional experiments are in Supp. Fig. 3. (B) Summary of IgG1 CSR levels of purified $CD43^-$ splenocytes after 4 days of anti-CD40 plus IL-4 stimulation. The y-axis shows the average percentage of $IgG1^+$ cells determined from multiple experiments with cells from WT (n=5), XLF $^{\Delta/\Delta}$(n=5), $ATM^{-/-}$(n=5), and $XLF^{\Delta/\Delta}ATM^{-/-}$HL(n=8) mice. Error bars show standard deviations; ***, $p<0.001$, based on student t-test between indicated pairs. (C) Percentage of direct junctions relative to direct plus MH-mediated junctions between Sμ and Sγ1 in anti-CD40 plus IL-4 stimulated B cells. Junctions were obtained from multiple independent experiments with XLF $^{\Delta/\Delta}$ (n=4), $ATM^{-/-}$(n=3), and $XLF^{\Delta/\Delta}ATM^{-/-}$HL (n=4) cells. See Sup. Fig. 4 for details.

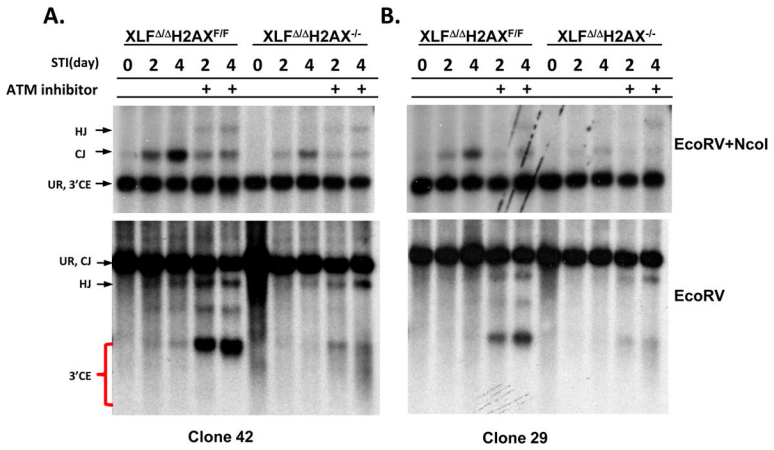

Figure 4. H2AX and XLF have redundant functions

(A and B) Southern blot analyses of rearrangement of clonally single intergrated pMX-INV inversional V(D)J recombination substrate in XLF$^{\Delta/\Delta}$H2AX$^{F/F}$ and derivative H2AX deleted XLF$^{\Delta/\Delta}$H2AX$^{-/-}$ lines. Clone 42 in panel A and Clone 29 in panel B. Upper: DNA was digested with EcoRV and NcoI and probed with C4 probe. Lower: DNA was digested with EcoRV and probed with C4 probe (see Fig. 1E and legend for additional details). Analysis of an independent line is presented in Sup. Fig. 5.

Table 1

H2AX and XLF have redundant functions in murine embryonic development

The Indicated genotypes were obtained by inter-crossing $H2AX^{+/-}XLF^{\Delta/\Delta}$ mice as described[5,12,22]. H2AX-deficiency does not cause embryonic lethality [22,27].

	H2AX+/+ XLFΔ/Δ	H2AX+/− XLFΔ/Δ	H2AX−/−XLFΔ/Δ	Absorbed	Total
Birth	14	46	0		60
Birth (exp)	15	30	15		
E13.5	8	28	0	8	44
E13.5(exp)	11	22	11		